CrossMark

Characterizing Aftershock Sequences of the Recent Strong Earthquakes in Central Italy

Vladimir G. Kossobokov[1,2,3,4] (iD) and Anastasia K. Nekrasova[1]

Abstract—The recent strong earthquakes in Central Italy allow for a comparative analysis of their aftershocks from the viewpoint of the Unified Scaling Law for Earthquakes, USLE, which generalizes the Gutenberg–Richter relationship making use of naturally fractal distribution of earthquake sources of different size in a seismic region. In particular, we consider aftershocks as a sequence of avalanches in self-organized system of blocks-and-faults of the Earth lithosphere, each aftershock series characterized with the distribution of the USLE control parameter, η. We found the existence, in a long-term, of different, intermittent levels of rather steady seismic activity characterized with a near constant value of η, which switch, in mid-term, at times of transition associated with catastrophic events. On such a transition, seismic activity may follow different scenarios with inter-event time scaling of different kind, including constant, logarithmic, power law, exponential rise/decay or a mixture of those as observed in the case of the ongoing one associated with the three strong earthquakes in 2016. Evidently, our results do not support the presence of universality of seismic energy release, while providing constraints on modelling seismic sequences for earthquake physicists and supplying decision makers with information for improving local seismic hazard assessments.

Key words: Unified scaling law for earthquakes, strong earthquakes, sequences of associated earthquakes, background seismic activity, self-organized non-linear dynamical system, control parameter of a system.

1. Introduction

Seismic reality evidences many contradictions to model assumption of a stationary Poisson point process (Gardner and Knopoff 1974) for analytically tractable testing the existing hypotheses. The assumption requires data adjustment and, by necessity, leads to complications: identification of main events and their fore- and aftershocks and introduction of hypothetical distributions of their size, inter-event time, and location. Therefore, estimation of earthquake recurrence at a given site remains the basic source of erroneous seismic hazard assessment and inflicted inadequate decisions (Kossobokov and Nekrasova 2012; Wyss et al. 2012; Davis et al. 2012; Panza et al. 2014; Nekrasova et al. 2014; Kossobokov et al. 2015).

The results of the global and regional analyses (Kossobokov and Mazhkenov 1994; Bak et al. 2002; Nekrasova and Kossobokov 2002, 2005, 2006, 2016; Kossobokov 2005; Nekrasova 2008; Nekrasova et al. 2011, 2015; Parvez et al. 2014) imply that the recurrence rate $N(M, L)$ of earthquakes of magnitude M within the range L, for a wide range of magnitudes $M \times (M_-, M_+)$ and sizes $L \times (L_-, L_+)$, can be described by the following formula:

$$N(M,L) = 10^A \times 10^{B \times (5-M)} \times L^C$$

where A, B, C are constants. A dual formulation using the inter-event time T instead of rate of occurrence N has been suggested by Bak et al. (2002) as Unified Scaling Law for Earthquakes, USLE. We keep using the name introduced by Per Bak (Bak et al. 2002; Christensen et al. 2002) for our generalization of Gutenberg–Richter relationship applied at a seismically prone site in the following form:

$$\log_{10} N(M,L) = A + B \times (5-M) + C \times \log_{10} L \quad (2)$$

where $N(M, L)$ is the expected annual number of earthquakes of a certain magnitude M within a seismically prone area of diameter L; A and B characterize the annual rate of magnitude 5 events and the balance between magnitude ranges, correspondingly, analogous to a- and b-values of the Gutenberg–Richter relationship (Gutenberg and

[1] Institute of Earthquake Prediction Theory & Mathematical Geophysics, RAS, Moscow, Russian Federation. E-mail: volodya@mitp.ru; nastia@mitp.ru
[2] Geophysical Center, RAS, Moscow, Russian Federation.
[3] Institut de Physique du Globe de Paris, Paris, France.
[4] International Seismic Safety Organization, Arsita, Italy.

Richter [1944](#), and C estimates the fractal dimension of the epicenter loci at the site.

2. Data and Methods

Seismicity of Central Italy is considered within 41°–44° N and 10°–15° E and 1995–2016. We work with the Parametric Catalogue of Italian Earthquakes (Catalogo Parametrico dei Terremoti Italiani, CPTI) of magnitude 3 or above (Gruppo di Lavoro [2004](#); Rovida et al. [2011](#)) updated from the online database of the INGV National Earthquake Center (http://cnt.rm.ingv.it/), which according to Fig. [1](#) provides a complete record of seismic activity in the Earth crust of the study area. The Gutenberg–Richter plot on the left, i.e., the cumulative number of earthquakes of magnitude M or above, follows

the exponential best fit trend-line with the slope (b-value) of 0.912 and $R^2 = 0.996$. Interestingly, the survival curve of the hypocenter depth fits the power law scaling with exponent -3.39 and $R^2 = 0.982$. According to the global ANSS Comprehensive Earthquake Catalog, there are five strong earthquakes of magnitude 6 or larger listed in Table [1](#), which magnitudes differ from those of CPTI. The discrepancy is quite within intrinsic accuracy of earthquake magnitude determinations, so that our choice of strong earthquakes for the study appears to be rather natural.

Figure [2](#) shows the map of epicenters of earthquakes in 1995–2016 (those of the five strong are marked with red dots). Figure [3](#) provides 3-D distribution of earthquakes by plots of magnitude versus time (top) and distance in km along NW strike (bottom).
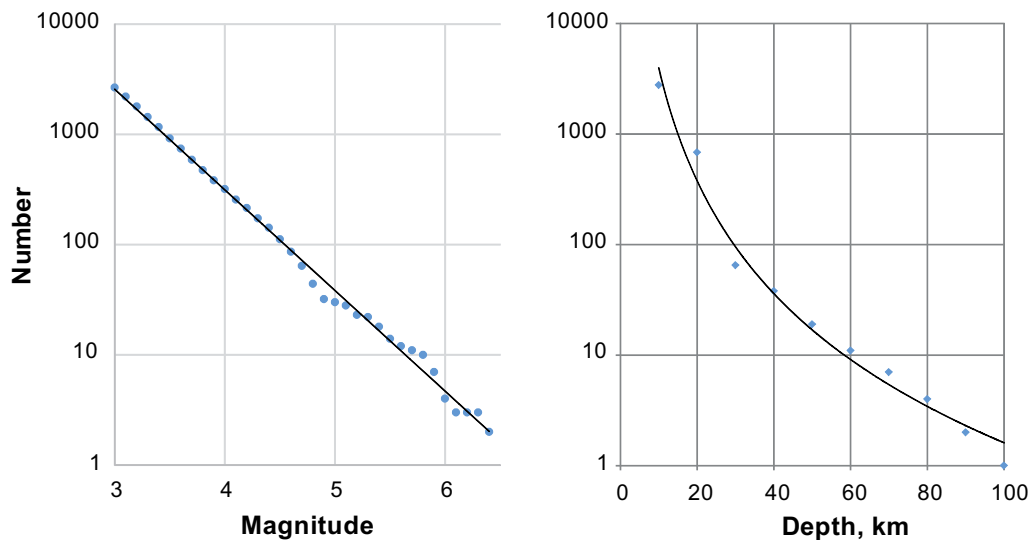

Figure 1

Cumulative number of earthquakes above certain magnitude (*left*) or shallower than a certain depth (in km, *right*) in Central Italy, 1995–2016

Table 1

Strong earthquakes in Central Italy, 1995–2016

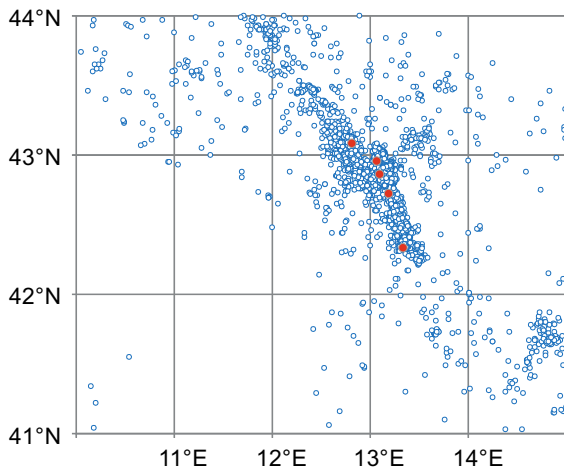| Origin time	Latitude	Longitude	Depth	M_{wGCMT}	M_{INGV}	Location
1997/09/26 09:40:26.3	43.084	12.812	10.0	6.0	6.4	4 km SSE of Nocera Umbra
2009/04/06 01:32:39.0	42.334	13.334	8.8	6.3	6.3	6 km W of L'Aquila
2016/08/24 01:36:32.9	42.723	13.188	4.4	6.2	6.0	5 km SWW of Amatrice
2016/10/26 19:18:08.4	42.956	13.067	10.0	6.1	5.9	3 km NNW of Visso
2016/10/30 06:40:18.7	42.862	13.096	8.0	6.6	6.5	7 km N of Norcia

Figure 2
Epicenters of earthquakes of magnitude 3 or above

We calculate the inter-event times (τ, in days) and plot them versus origin time (Fig. 4) along with the 25 events moving average trend-line (red curve). By a visual inspection of Figs. 3 and 4, we observe clustered irregularity of seismic dynamics in the study area: sparse distribution in space and time before the 2009 L'Aquila earthquake characterized with the aftershock series of the 1997 Umbria and Marche and 2002 Molise earthquakes (at the most south-eastern periphery of the study area), otherwise, average recurrence of about one magnitude 3 or larger in ten or more days and much more higher clustered activity after 2009 in advance of the triple strong earthquakes in the second half of 2016. The trend-line marks revival of activity within a year by characteristic oscillations in March 1998, in case of the 1997 Umbria and Marche earthquake, and in July, October 2009, and January 2010 in case of the 2009 L'Aquila earthquake. Zooming on the strong earthquake origin times (Fig. 5) discloses evidently different rise of inter-event time, dual to different decay of the aftershock number in contradiction to the classical Omori law (Omori 1894): near constant for about 20 days in October 1997, power in 6–9 April 2009 ($\tau = 0.0211t^{0.8031}$, $R^2 = 98.84\%$), exponential in 10–24 April 2009 ($\tau = 0.0244e^{0.1471t}$, $R^2 = 97.52\%$), and, perhaps, a mixture of the four model kinds of inter-event time rise in September–December
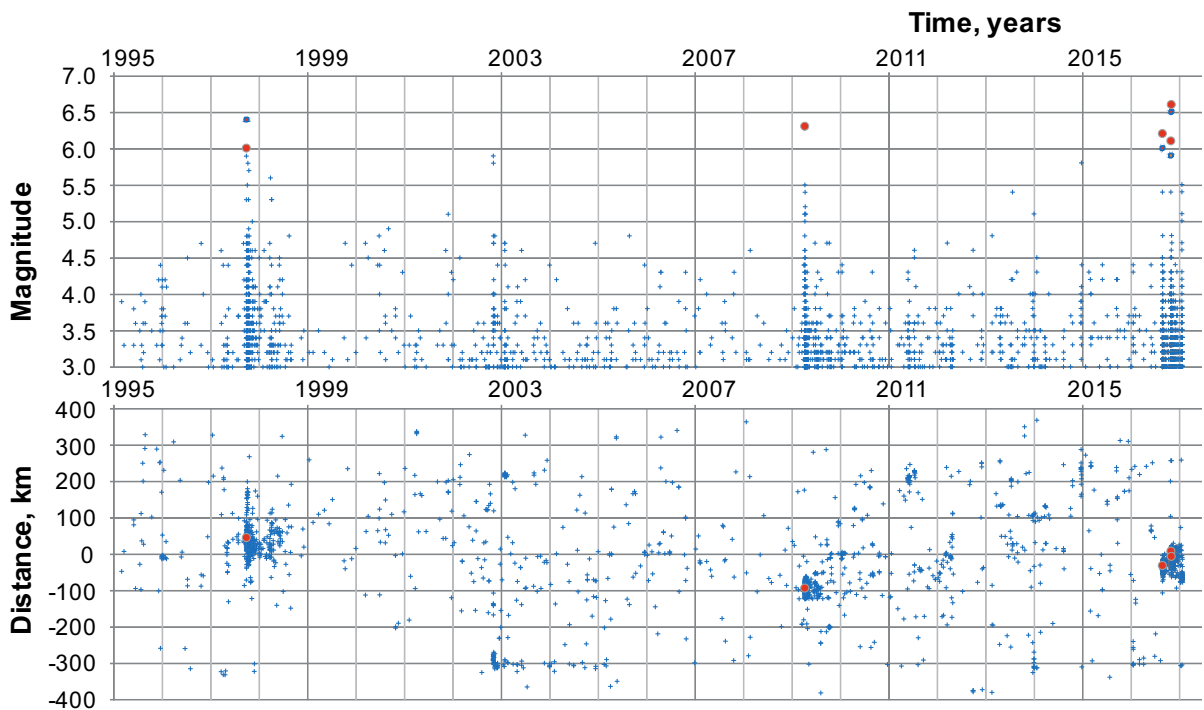

Figure 3
Magnitude–space–time distribution of earthquakes in Central Italy. The five strong earthquakes are marked with *red dots*, in particular, with larger dots for M_{wGCMT} and *smaller dots* for M_{INGV} on the magnitude versus time plot (*top frame*)
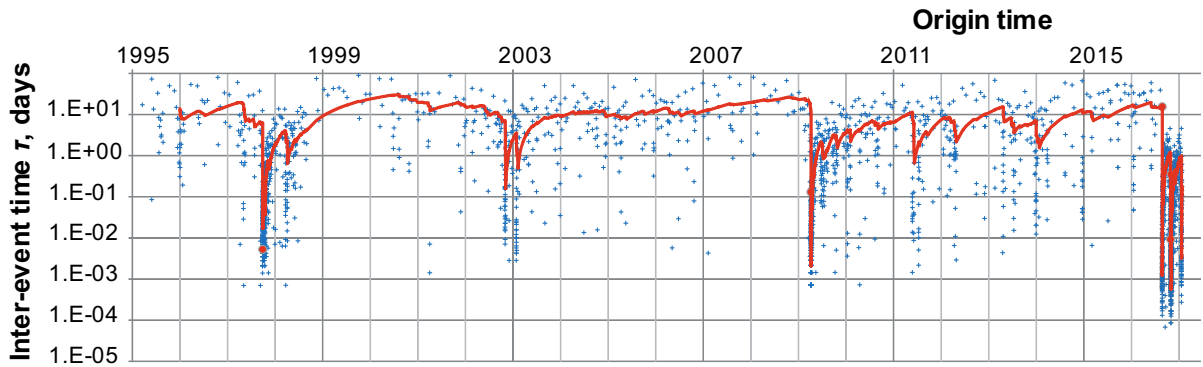
Figure 4
The inter-event time τ (in days) versus the earthquake origin time in Central Italy (since 1995)
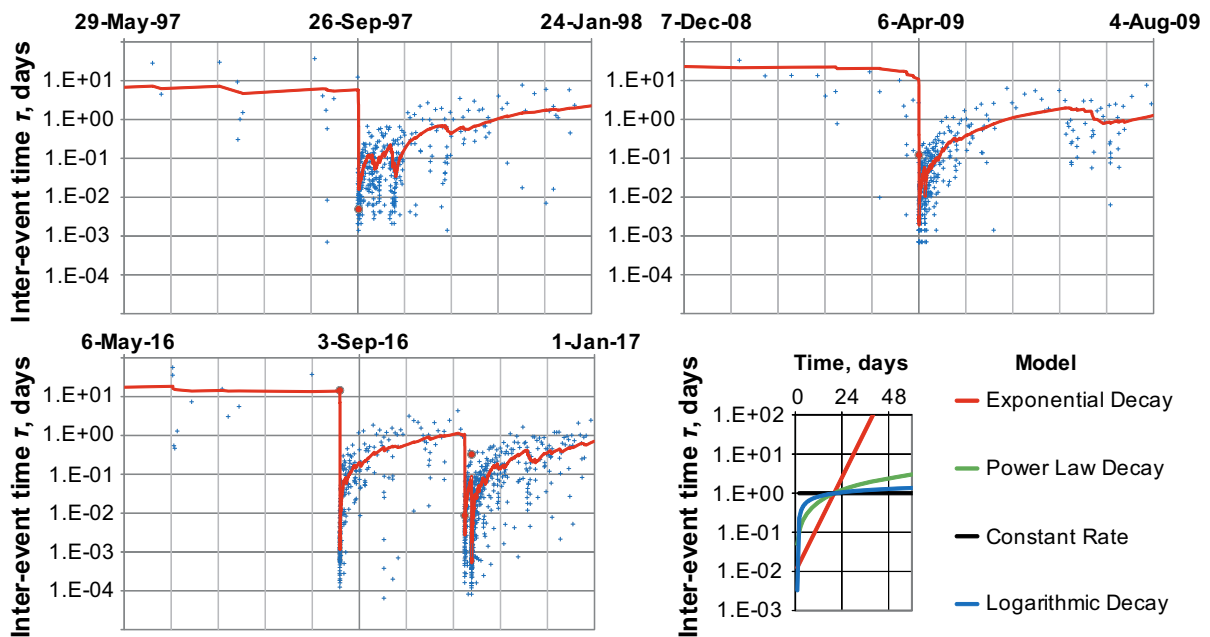

Figure 5
The inter-event times in advance and after the strong earthquakes

2016. Table 2 sums up the best fit approximations of the 25 event moving average of inter-event times for each of the five aftershock series during the first 24 days after the main shock in assumption of exponential, linear, logarithmic, or power law rise. Table 3 provides the Akaike Information Criterion (AIC) values for the best fit of the aftershock rate within the first 60 days after each of the five main shocks according to the SASeis AFT by Utsu and Ogata (1997). The SASeis package including in detail descriptions and source codes of 10 programs for statistical analysis of

seismicity is available from the International Association of Seismology and Physics of the Earth's Interior (IASPEI) Software Library. The SASeis AFT program computes the maximum likelihood estimates of the parameters in several selected equations which represent the decay laws of the aftershock occurrence rate, along with the AIC values and provides the graphs of the best fit rate and cumulative-frequency curves with the input data points. The maximum of R^2 in Table 2 and the minimum of the AIC values in Table 3 confirm quantitatively the diversity of seismic activity decay

Table 2

The best fit approximations of the 25 event moving average of inter-event times during the first 24 days after the main shock

	Exponential $aexp^{bt}$	Linear $at + b$	Logarithmic $aln(t) + b$	Power at^b
UM				
a	0.0399	0.0032	0.0254	0.029
b	0.0495	0.0477	0.0321	0.4375
R^2	30.03%	23.96%	36.71%	**55.83%**
AQ				
a	0.0128	0.0146	0.0361	0.0181
b	0.1975	−0.0076	0.0349	0.7639
R^2	73.49%	**93.44%**	47.92%	91.46%
AM				
a	0.0076	0.0188	0.0464	0.0227
b	0.2504	0.0042	0.0876	0.9511
R^2	62.55%	98.35%	66.00%	**99.31%**
VI				
a	0.0080	0.0211	0.0162	0.0250
b	0.8319	0.0028	0.0304	0.7839
R^2	82.78%	**98.41%**	76.78%	97.63%
NO				
a	0.0047	0.0113	0.0255	0.0129
b	0.2585	0.0005	0.0447	0.9007
R^2	66.35%	97.15%	60.16%	**98.54%**

Note: The maximal value of R^2 that characterizes the best fit model for each main shock is given in bold

scenarios after the strong earthquakes in Central Italy. Let us investigate in more detail, the five aftershock series by applying techniques based on USLE.

3. Application of the USLE-Based Methods

We take the values of the USLE coefficients from the maps for the entire territory of Italy compiled recently by Nekrasova (2013) making use of the CPTI long-term data. Specifically, in the following computations we use the values of B and

C coefficients, analogous to the b-value and d_f of Bak et al. (2002), mapped in Fig. 6 and listed for locations of the five strong earthquakes in Table 4.

From a physical viewpoint, the scaling parameter $10^{B \times (5-M)} \times L^C / N$ of USLE, analogous to $TS^{-b}L^{df}$, where T is inter-event time and $\log_{10}(S) = M$ (Bak et al. 2002; Christensen et al. 2002), controls self-organized non-linear seismic system of a given region, so that the distribution of inter-event times depends only on this parameter. In Fig. 7, we plot the distribution of the control parameter value $\eta = \tau \times 10^{B \times (5-M)} \times L^C$ for each earthquake in the study area and the 25-event moving average trend-line of this control parameter of seismic activity in Central Italy. Evidently, Figs. 7 and 8 appear very similar to Figs. 4 and 5; however, the trend-line for η, which can be viewed as a short-term estimation of the A coefficient of USLE, is more consistent (more smooth, less spiky) than that for τ. Naturally, (a) when the trend-line for η goes above a certain threshold ($\eta = 1$, i.e., expectation of about 1 event of magnitude 5 in a year), earthquakes become less clustered in space and time, and (b) strong earthquakes mark the times of transition from a stable level of η to a different stable level (specifically, we find the 25-event moving average of η at about 22.03 ± 9.42 in 1996–June 1997, 20.14 ± 6.79 in 1999–June 2002, 17.81 ± 5.31 in 2004–2008, and 8.12 ± 4.56 in 2010–May 2016), well in line of behavior at the times of critical transitions in self-organized non-linear systems (Bak and Tang 1989).

Expanding application of the USLE, Baiesi and Paczuski (2004) introduced the space–time–magnitude proximity η_{ij} between any two earthquakes i and j based on the control parameter $\eta = \eta_{i(i-1)}$. The

Table 3

The values of AIC for the SASeis AFT (Utsu and Ogata 1997) best fit model approximations of the rate of the five aftershocks during the first 60 days after the main shock

	Exponential $B + kexp^{-qt}$	Omori $B + k/(t + c)$	Modified Omori $B + k/(t + c)^p$	Weibull $B + kt^{(b-1)}exp^{-at**b}$
UM	−743	−745	−745	**−761**
AQ	−1198	−1295	−1296	**−1341**
AM	−1066	−1164	**−1165**	−1145
VI	**−3011**	−2874	−2973	−2947
NO	−2988	**−3152**	−3151	−3114

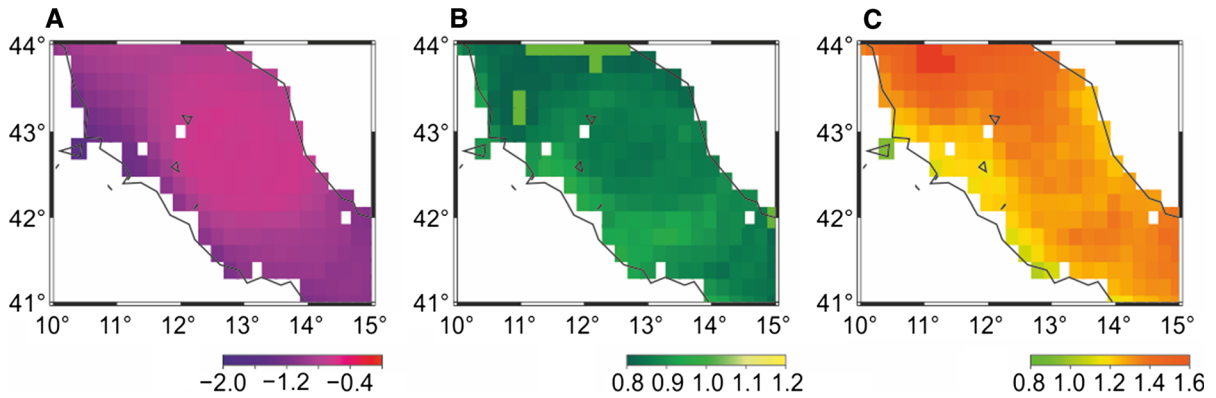Note: The minimal value of AIC that characterizes the best fit model for each main shock is given in bold

Figure 6
The maps of the estimates of the USLE coefficients *A, B,* and *C* in the study area (Nekrasova 2013)

Table 4

The USLE coefficients at the five epicenters

Earthquake name	Latitude	Longitude	A	B	C
1997 Umbria and Marche	43.084	12.812	−0.621	0.867	1.380
2009 L'Aquila	42.334	13.334	−0.622	0.866	1.333
2016 Amatrice	42.723	13.188	−0.624	0.859	1.311
2016 Visso	42.956	13.067	−0.624	0.847	1.327
2016 Norcia	42.862	13.096	−0.618	0.844	1.323

properties of this proximity measure with physical motivations for cluster analysis of seismic phenomena at regional and global scales are discussed at length in (Zaliapin et al. 2008; Zaliapin and Ben-Zion 2013, 2015, 2016). In particular, Ilya Zaliapin developed the *Matlab* code for problem-oriented presentation of clustering properties of earthquakes, which we have an opportunity to apply to seismicity

within 100 km distance from the epicenter and 60 days after the origin time of each of the five strong earthquakes in Central Italy (in case of the 26 October 2016 Visso earthquake the sample is limited by the origin time of the 30 October 2016 Norcia earthquake). Figure 9 displays density and cumulative distributions of the control parameter η for these five samples of earthquakes, which are significantly different except for the two out of ten pairs, i.e., L'Aquila-Amatrice (AQ-AM) and Amatrice-Norcia (AM-NO) (Table 5). Figure 10 presents the distribution of the joint two-dimensional density of (R, T), which normalized space, $R_{ij} = \rho_{ij} \times 10^{-C \times p \times Mi}$ (where ρ_{ij} is the distance between earthquakes i and j) and time, $T_{ij} = \tau_{ij} \times 10^{-B \times q \times Mi}$, components get equal weights from η_{ij} earthquake sizing ($q = p = 0.5$). Color scales on the right represent the relative number of points, so that the integral over the
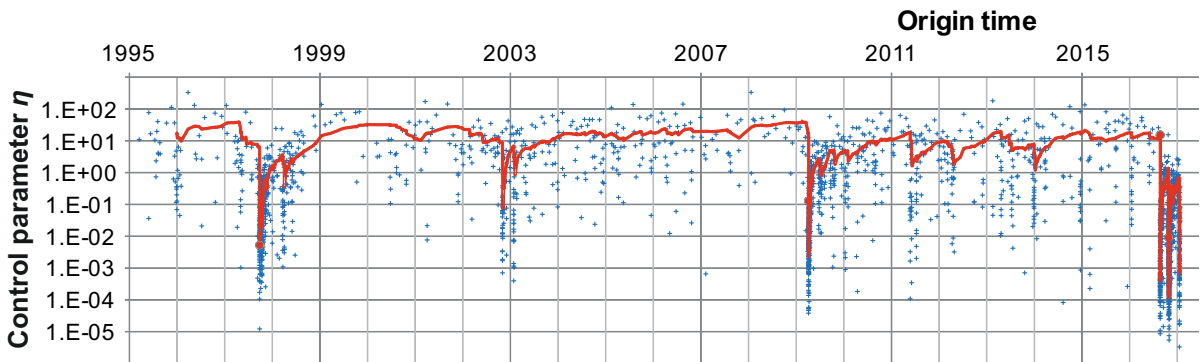

Figure 7
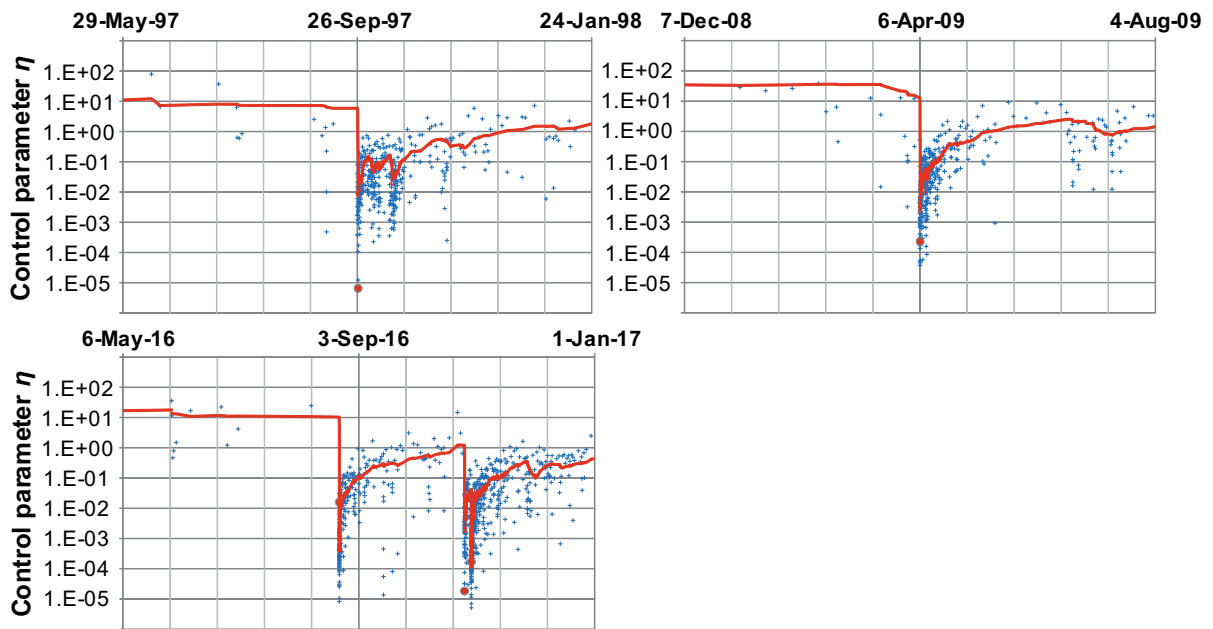The control parameter $\eta = \tau \times 10^{B \times (5-M)} \times L^{C}$ versus the origin time

Figure 8

The control parameter $\eta = \tau \times 10^{B \times (5-M)} \times L^{C}$ versus the origin time in advance and after strong earthquakes in Central Italy, 1995–2016
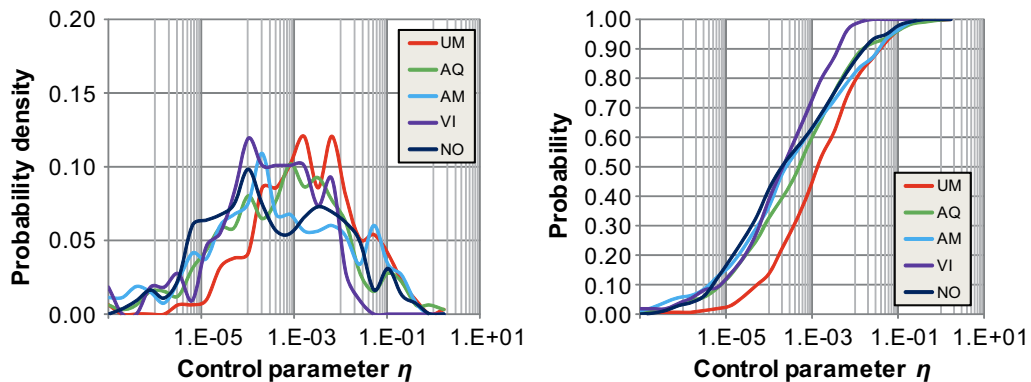

Figure 9

The density (*left*) and cumulative (*right*) distributions of the control parameter η for the five aftershock series in Central Italy, 1995–2016. The integral over each of the five density distributions equals 1; (UM) 1997 Umbria and Marche, (AQ) 2009 L'Aquila, (AM) 2016 Amatrice, (VI) 2016 Visso, and (NO) 2016 Norcia

entire distribution is 1. For the purposes of comparison, the right panel at the bottom displays the contours of 0.2 density levels from all the five cases, which indicate the differences and similarities of the aftershock series. Specifically, (i) the outlines have a common intersection, (ii) the 1997 Umbria and Marche series has a larger than other's span along *R*, (iii) the 2009 L'Aquila series in addition to double peak hill, similar to that of the 2016 Amatrice, at

rescaled distances in the order of 10^{-2} has an outlier at small rescaled distances of about 10^{-5}, (iv) the outlines of the 2016 triple are concentric and correlate to the earthquake size (specifically, the span of the rescaled distance, ΔR, of the 0.2 outlines correlates perfectly well to the characteristic length e^{M} of the corresponding three strong earthquake sources: correl(ΔR, e^{M}) = 99.94%).

Table 5

The Kolmogorov–Smirnov two-sample λ_{KS}-test results for the pairs of distributions of the control parameter η in the five aftershock series in Central Italy, 1995–2016

	UM	AQ	AM	VI	NO
UM	315	2.60	3.10	2.88	4.27
AQ	1.96E−06	324	*1.24*	1.52	1.73
AM	6.02E−09	*0.0793*	266	1.73	*0.93*
VI	8.87E−08	0.0169	0.0040	109	1.54
NO	1.91E−16	0.0043	*0.3234*	0.0149	549

The λ_{KS} values are given above the diagonal, the sample sizes—on the diagonal, and the probabilities of the two samples belonging to the same distribution (i.e., the statistical significance levels)—below the diagonal; the statistics are given in italics, if the two distributions are NOT significantly different at the 0.05 level

4. Discussion and Conclusions

Seismic evidences accumulated to date demonstrate clearly that most of the empirical relations commonly accepted in the early history of instrumental seismology can be proved erroneous when testing statistical significance is applied (Utsu et al. 1995; Bak et al. 2002; Kossobokov and Romashkova 2005; Ben-Zion 2008; Kossobokov et al. 2008; Zaliapin et al. 2008; Kossobokov and Nekrasova 2012; Panza et al. 2014; Davidsen et al. 2015; Mignan 2015; Zaliapin and Ben-Zion 2016; Nava et al. 2017). Earthquakes cascade into aftershocks that readjust the hierarchical system of blocks-and-faults in the locality of the main shock rupture. Our study attempts contributing to better understanding of seismic process considered from the viewpoint of non-linear dynamics of naturally fractured system of blocks-and-faults (Okubo and Aki 1987; Keilis-Borok 1990; Keilis-Borok and Soloviev 2003). The redistribution of energy in seismic system from the main shock down the hierarchy is studied for more than a century (Omori 1894; Utsu et al. 1995). However, the model power law decay of the aftershock activity is rarely followed in reality (Lepreti et al. 2009; Mignan 2015). For example, the majority of the great, magnitude 8 or larger earthquakes show switching to higher activity level of recurrence; their aftershock number differs by factor 100 or more and their relaxation time varies up to 50 times (Romashkova et al. 2000). This is in agreement with the recent studies of earthquake clustering on a global

scale by Zaliapin and Ben-Zion (2016), who conclude that "seismicity clusters have spatially dependent distribution, tightly correlated with the global heat flow production". The observed seismic diversity appears to be at the core of the recent debate about the rejection of the Omori law by a better fit Weibull (stretched exponential), exponential, or power law models (Mignan 2015, 2016a, b; Hainzl and Christophersen 2016). Clear patterns in space–time-energy distribution of earthquakes, as well as consecutive stages of direct and inverse cascading after and prior to main shocks, have been reported earlier (e.g., Reasenberg 1985; Bak and Tang, 1989; Davis and Frohlich 1991; Bufe and Varnes 1993; Kossobokov and Romashkova 2005, Ben-Zion 2008; Davidsen et al. 2015): the first may reflect readjustment of a complex system of blocks-and-faults in a new state after a catastrophe, while the second may indicate coalescence of instabilities at the approach of it. Analyzing variability of seismic activity at a regional scale, Nekrasova et al. (2011) have demonstrated a complex distribution of the USLE coefficients *A, B,* and *C* in Italy, which do not display any evident general correlation, although following well-organized attractor in the 3D domain of possible values. Notably, the analysis of inter-event time distributions of aftershocks of some strong seismic events in Southern California in comparison to those of solar flares in certain flare productive regions (Kossobokov et al. 2008) has shown that the two phenomena have different statistics of scaling, and even the same phenomenon, when observed in different periods or at different locations, is characterized by different statistics that cannot be uniformly rescaled onto a single, universal curve.

The sequence of strong, magnitude 6 or above earthquakes in Central Italy provides a unique opportunity for a comparative analysis of the well-documented aftershock series from approximately the same area and even time: the epicentres of the five strong earthquakes in 1997–2016 are within 100 km distance from each other, whereas the last three earthquakes in 2016—within less than 30 km distance. The results of our study are tested to be robust and do not change qualitatively by variation of parameters in computations (i.e., magnitude cutoff, sample size of the moving average, etc.). Our analysis
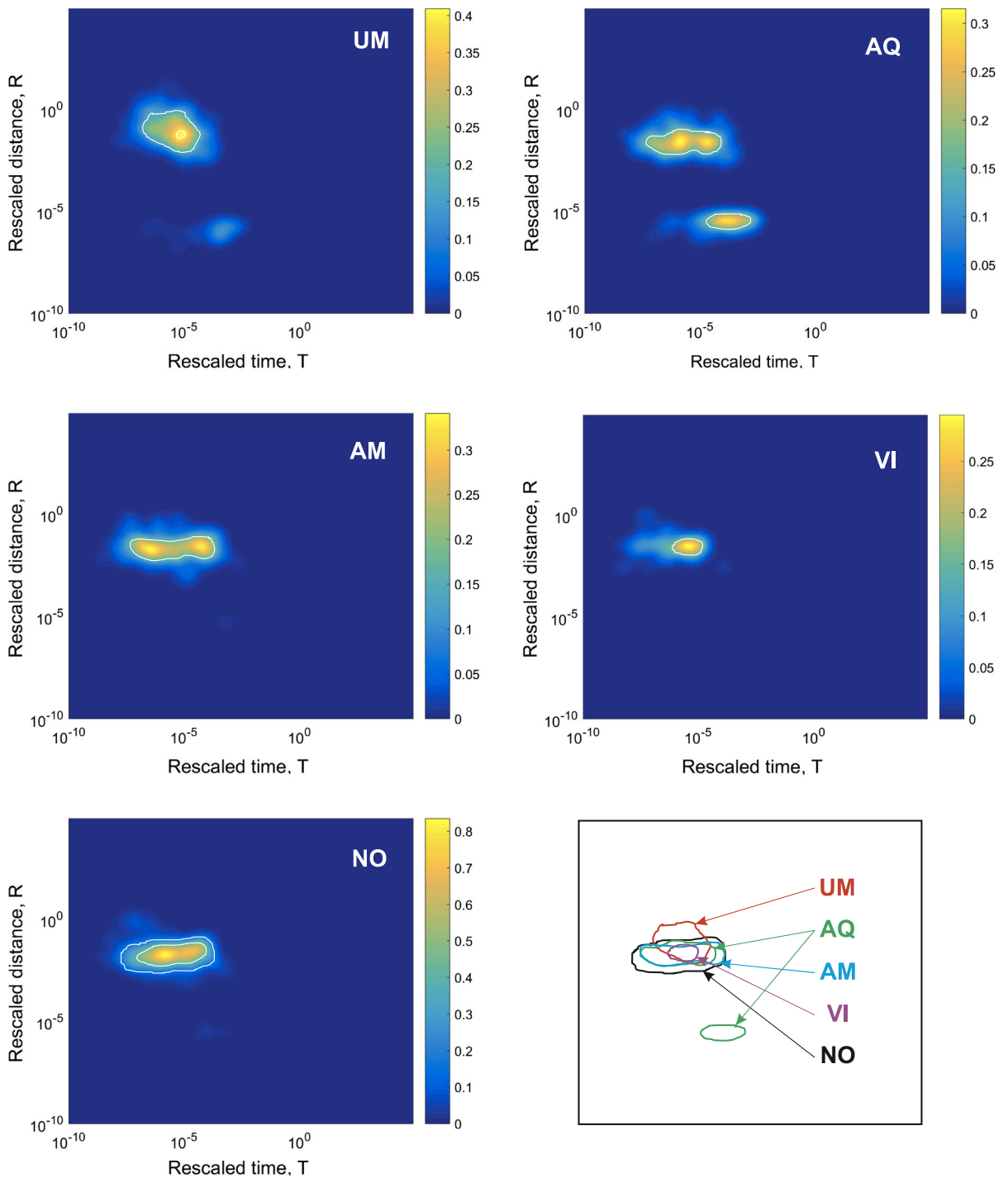
Figure 10
The two-dimensional density distributions of the $\eta = R \times T$ components of rescaled distance and time (R, T) for the five aftershock series in Central Italy, 1995–2016. The integral over each of the five distributions equals 1; (UM) 1997 Umbria and Marche, (AQ) 2009 L'Aquila, (AM) 2016 Amatrice, (VI) 2016 Visso, and (NO) 2016 Norcia; (*bottom*, *right*) the density outlines at 0.2 level for all the five cases together

of space–time-energy distributions of seismic activity in Central Italy confirms the existence of different, intermittent levels of rather long-term steady seismic activity characterized with a near constant value of the USLE control parameter η. The region switches from one level to another one in a shorter-term transition associated with strong, catastrophic events. During such a switch, seismic activity may follow very different scenarios with inter-event scaling of different kind, such as constant, logarithmic, power law, exponential rise/decay or a mixture of those as observed in the case of the 2016 strong earthquakes. Evidently, our results do not support the presence of universality in seismic energy release. The observed variability of seismic activity provides important constraints on modeling earthquake sequences by geophysicists and can be used to improve local seismic hazard assessments including those of earthquake forecast/prediction techniques (Nekrasova and Kossobokov 2005; Kossobokov 2013). The transition of seismic regime in Central Italy started in 2016 is not over yet and requires special attention. It would be premature to make any kind of definitive conclusions on the level of seismic hazard which is evidently high at this particular moment of time.

Acknowledgements

REFERENCES

Baiesi, M., & Paczuski, M. (2004). Scale-free networks of earthquakes and aftershocks. *Physical Review E, 69,* 066106. doi:10.1103/PhysRevE.69.066106.

Bak, P., Christensen, K., Danon, L., & Scanlon, T. (2002). Unified scaling law for earthquakes. *Physical Review Letters, 88,* 178501–178504.

Bak, P., & Tang, C. (1989). Earthquakes as a self-organized critical phenomenon. *Journal of Geophysical Research, 94,* 15635–15637.

Ben-Zion, Y. (2008). Collective behavior of earthquakes and faults: continuum-discrete transitions, progressive evolutionary changes, and different dynamic regimes. *Revues of Geophysics, 46*(4), RG4006. doi:10.1029/2008RG000260.

Bufe, C. G., & Varnes, D. J. (1993). Predictive modeling of the seismic cycle of the greater San Francisco Bay region. *Journal of Geophysical Research, 98,* 9871–9883.

Christensen, K., Danon, L., Scanlon, T., & Bak, P. (2002). Unified scaling law for earthquakes. *Proceedings of the National Academy of Sciences, 99*(suppl 1), 2509–2513.

Davidsen, J., Gu, C., & Baiesi, M. (2015). Generalized Omori-Utsu law for aftershock sequences in southern California. *Geophysical Journal International, 201*(2), 965–978.

Davis, S. D., & Frohlich, C. (1991). Single link cluster analysis of the earthquake aftershocks: decay laws and regional variations. *Journal of Geophysical Research, 96,* 6335–6350.

Davis, C., Keilis-Borok, V., Kossobokov, V., & Soloviev, A. (2012). Advance prediction of the March 11, 2011 Great East Japan Earthquake: A missed opportunity for disaster preparedness. *International Journal of Disaster Risk Reduction, 1,* 17–32. doi:10.1016/j.ijdrr.2012.03.001.

Gardner, J., & Knopoff, L. (1974). Is the sequence of earthquakes in S. California with aftershocks removed Poissonian? *Bulletin of the Seismological Society of America, 64*(5), 1363–1367.

Gruppo di Lavoro (2004). *Catalogo parametrico dei terremoti italiani, versione 2004 (CPTI04).* INGV, Bologna. http://emidius.mi.ingv.it/CPTI04/.

Gutenberg, B., & Richter, C. F. (1944). Frequency of earthquakes in California. *Bulletin of the Seismological Society of America, 34*(4), 185–188.

Hainzl, S., & Christophersen, A. (2016). Comment on Revisiting the 1894 Omori aftershock dataset with the stretched exponential function by A. Mignan. *Seismological Research Letters, 87,* 1130–1133. doi:10.1785/0220160098.

Keilis-Borok, V. I. (1990). The lithosphere of the Earth as a nonlinear system with implications for earthquake prediction. *Reviews of Geophysics, 28*(1), 19–34.

Keilis-Borok, V. I., & Soloviev, A. A. (Eds.). (2003). *Nonlinear dynamics of the lithosphere and earthquake prediction* (p. 337). Heidelberg: Springer.

Kossobokov, V.G. (2005). *Earthquake prediction: Principles, implementation, perspectives, in: Earthquake prediction and geodynamic processes.* (Computational Seismology, Issue 36, Part 1), Moscow, GEOS **(in Russian)**.

Kossobokov, V. G. (2013). Earthquake prediction: 20 years of global experiment. *Natural Hazards, 69*(2), 1155–1177. doi:10.1007/s11069-012-0198-1.

Kossobokov, V. G., Lepreti, F., & Carbone, V. (2008). Complexity in sequences of solar flares and earthquakes. *Pure and Applied Geophysics, 165,* 761–775. doi:10.1007/s00024-008-0330-z.

Kossobokov, V. G., & Mazhkenov, S. A. (1994). On similarity in the spatial distribution of seismicity. In D. K. Chowdhury (Ed.), *Computational Seismology and Geodynamics, 1* (pp. 6–15). Washington DC: AGU, The Union.

Kossobokov, V., & Nekrasova, A. (2012). Global seismic hazard assessment program maps are erroneous. *Seismic Instruments, 48*(2), 162–170. doi:10.3103/S0747923912020065.

Kossobokov, V., Peresan, A., & Panza, G. F. (2015). Reality check: seismic hazard models you can trust. *EOS, 96*(13), 9–11.

Kossobokov, V. G., & Romashkova, L. L. (2005). Seismicity dynamics prior to and after the largest earthquakes worldwide, 1985–2000. In D. K. Chowdhury (Ed.), *Computational seismology and geodynamics* (Vol. 7, pp. 138–160). Washington D.C.: AGU.

Lepreti, F., Kossobokov, V. G., & Carbone, V. (2009). Statistical properties of solar flares and comparison to other impulsive energy release events. *International Journal of Modern Physics B, 23*(28–29), 5609–5618.

Mignan, A. (2015). Modeling aftershocks as a stretched exponential relaxation. *Geophysical Research Letters, 42,* 9726–9732. doi:10.1002/2015GL066232.

Mignan, A. (2016a). Revisiting the 1894 Omori aftershock dataset with the stretched exponential function. *Seismological Research Letters*. doi:10.1785/0220150230.

Mignan, A. (2016b). Reply to "Comment on 'Revisiting the 1894 Omori Aftershock Dataset with the Stretched Exponential Function' by A. Mignan" by S. Hainzl and A. *Christophersen, Seismological Society of America, 87,* 1134–1137. doi:10.1785/0220160110.

Nava, F. A., Marquez-Ramırez, V. H., Zuniga, F. R., & Lomnitz, C. (2017). Gutenberg-Richter b-value determination and large-magnitudes sampling. *Natural Hazards, 87,* 1–11. doi:10.1007/s11069-017-2750-5.

Nekrasova, A.K. (2008). *Unified Scaling Law for Earthquakes: Application to seismically active regions of the world.* (PhD. thesis), M.V. Lomonosov Moscow State University, Moscow. **(in Russian)**.

Nekrasova, A.K. (2013). Estimation of seismic hazard and risks for Italy based on Unified scaling law for earthquakes. *ICTP Interim Report*, Miramare–Trieste, September 2013.

Nekrasova, A. K., & Kosobokov, V. G. (2006). Unified scaling law for earthquakes in the Lake Baikal region. *Doklady Earth Sciences, 407A*(3), 484–485.

Nekrasova, A. K., & Kosobokov, V. G. (2016). Unified scaling law for earthquakes in Crimea and Northern Caucasus. *Doklady Earth Sciences., 470*(2), 1056–1058.

Nekrasova, A., & Kossobokov, V. (2002). Generalizing the Gutenberg–Richter scaling law. *EOS Trans AGU., 83*(47), 62–0958.

Nekrasova, A. K., & Kossobokov, V. G. (2005). Temporal variations in the parameters of the Unified Scaling law for earthquakes in the eastern part of Honshu Island (Japan). *Doklady Earth Sciences, 405,* 1352–1356.

Nekrasova, A., Kossobokov, V., Parvez, I. A., & Tao, X. (2015). Seismic hazard and risk assessment based on the unified scaling law for earthquakes. *Acta Geodaetica et Geophysica, 50*(1), 21–37. doi:10.1007/s40328-014-0082-4.

Nekrasova, A., Kossobokov, V., Perezan, A., Aoudia, A., & Panza, G. F. (2011). A multiscale application of the Unified scaling law for earthquakes in the Central Mediterranean area and Alpine region. *Pure and Applied Geophysics, 168,* 297–327. doi:10.1007/s00024-010-0163-4.

Nekrasova, A., Peresan, A., Kossobokov, V.G. & Panza, G.F. (2014). Chapter 7: A new probabilistic shift away from seismic hazard reality in Italy? In: Aneva, B. & Kouteva-Guentcheva, M. (Eds.), *Nonlinear Mathematical Physics and Natural Hazards, Springer Proceedings in Physics*, 163, 83–103. http://dx.doi.org/10.1007/978-3-319-14328-6_7.

Okubo, P. G., & Aki, K. (1987). Fractal geometry in the San Andreas fault system. *Journal of Geophysical Research, 92,* 345–355.

Omori, F. (1894). On after-shocks of earthquakes. *Journal of the College of Science, Imperial University of Tokyo, 7,* 111–200.

Panza, G. F., Kossobokov, V., Peresan, A., & Nekrasova, A. (2014). Chapter 12. Why are the standard probabilistic methods of estimating seismic hazard and risks too often wrong? In M. Wyss & J. Shroder (Eds.), *Earthquake Hazard, Risk, and Disasters* (pp. 309–357). London: Elsevier.

Parvez, I. A., Nekrasova, A., & Kossobokov, V. (2014). Estimation of seismic hazard and risks for the Himalayas and surrounding regions based on unified scaling law for earthquakes. *Natural Hazards, 71*(1), 549–562. doi:10.1007/s11069-013-0926-1.

Reasenberg, P. (1985). Second-order moment of Central California seismicity, 1969–1982. *Journal of Geophysical Research, 90,* 5479–5495.

Romashkova, L., Kossobokov, V. & Turcotte, D. (2000). Seismic cascades prior to and after recent largest earthquakes worldwide. *Eos Trans. AGU*, 81 (48), Fall Meet. Suppl., Abstract NG62C-09, 2000: F564–F565.

Rovida, R. Camassi, P. Gasperini and M. Stucchi (eds.) (2011). *CPTI11, the 2011 version of the Parametric Catalogue of Italian Earthquakes*. Milano. http://emidius.mi.ingv.it/CPTI. Doi: 10.6092/INGV.IT-CPTI11.

Utsu, T., & Ogata, Y. (1997). Statistical analysis of seismicity. In: Healy, J.H., Keilis-Borok, V.I. & Lee, W.H.K. (Eds), *Algorithms for earthquake statistics and prediction.* IASPEI Software Library, Vol. 6. Seismol. Soc. Am., El Cerrito. pp. 13–94.

Utsu, T., Ogata, Y., & Matsuura, R. (1995). The centenary of the Omori formula for a decay law of aftershock activity. *Journal of Physics of the Earth, 43*(1), 1–33.

Wyss, M., Nekrasova, A., & Kossobokov, V. (2012). Errors in expected human losses due to incorrect seismic hazard estimates. *Natural Hazards, 62*(3), 927–935. doi:10.1007/s11069-012-0125-5.

Zaliapin, I., & Ben-Zion, Y. (2013). Earthquake clusters in southern California I: identification and stability. *Journal of Geophysical Research, 118*(6), 2847–2864.

Zaliapin, I., & Ben-Zion, Y. (2015). Artifacts of earthquake location errors and short-term incompleteness on seismicity clusters in southern, California. *Geophysical Journal International, 202,* 1949–1968.

Zaliapin, I., & Ben-Zion, Y. (2016). A global classification and characterization of earthquake clusters. *Geophysical Journal International, 207,* 608–634.

Zaliapin, I., Gabrielov, A., Keilis-Borok, V., & Wong, H. (2008). Clustering analysis of seismicity and aftershock identification. *Physical Review Letters, 101,* 018501. doi:10.1103/PhysRevLett.101.018501.